

# Noncoherent Multi-user Detection with a Receive Antenna Array for Fading Channels

Michael L. McCloud, Artur Russ, Louis L. Scharf, and Mahesh K. Varanasi<sup>1</sup>

*Abstract* — We consider M-ary communication with  $K$  users over a space diversity channel, consisting of a single transmit antenna and multiple receive antennas. We examine two different flat fading models, namely phase coherent wavefront fading and noncoherent element-to-element fading. In the case of wavefront fading, the fade is constant across the face of the receive antenna and we can associate an angle of arrival to the signal. In the case of non-coherent element-to-element fading, the fading path to each sensor is different (although possibly correlated) and no angle of arrival can be exploited for beamforming. For each channel model we develop several detection strategies which assume various amounts of prior information about the fading.

## I. INTRODUCTION

M-ary modulation schemes are commonly employed on noncoherent channels. The IS-95 standard, for example, employs Walsh codes on the uplink of the channel, which are decoded noncoherently. This is just one example of orthogonal multipulse modulation and noncoherent frequency shift keying is another. Other common techniques employ differential phase encoding and then perform detection by processing the received data two symbols at a time. The effective model employed in such detection is of an  $M^2$ -ary constellation with each two dimensional transmit vector corresponding to the present and previous information symbol (see e.g. [1]).

In this paper we consider several extensions of the noncoherent multiuser detection results of [2]-[4] for M-ary communication to the multiple antenna fading channel. We consider two basic channel models. In the first case, the fading process for each user is assumed constant across the face of the array. This is called coherent wavefront fading. The second model we consider is the noncoherent element-to-element fading channel on which each sensor receives a copy of the transmitted signal with a different fading parameter. The fading coefficients may be correlated on this channel.

For the coherent wavefront fading channel, we are able to associate a direction of arrival (DOA) with each user and employ detection rules which exploit this structure. The detection schemes are extensions of the generalized maximum likelihood (GML) and the minimum mean squared error (MMSE)

detectors presented in [2]-[5], the main difference being the inclusion of the DOA.

In Section IV we introduce two detection strategies for the noncoherent element-to-element fading channel, each appropriate for a different set of assumptions about the fading. We first develop a GML detector under the assumption of unknown deterministic fading. This technique is also appropriate for Rayleigh fading when the spatial correlation of the fading process is unknown (or the fading is assumed independent and identically distributed across the array). The detector acts to completely cancel multiple access interference, making it a zero-forcing invariant detector.

The MMSE detector rule requires knowledge of the fading correlation for the user of interest. By examining the asymptotic algebraic structure of the MMSE detector we find a zero-forcing detector which is an analog to the multipulse decorrelating (MD) detector presented in [4] (for the case of binary signalling, an optimality of an equivalent detector was proved earlier in [6]). The MD detector does not require knowledge of the fading correlations.

The performance of each detector is analyzed through the use of a union upper bound on the symbol error probability. It is shown that each detector achieves the expected dependency on the signal-to-noise ratio (i.e.  $(1/SNR)$  for the wavefront fading channel and  $(1/SNR)^L$  for the element-to-element fading channel) so long as there is some separation between the signal subspace and the interference subspaces of the other users.

## II. THE ANTENNA ARRAY MODEL WITH MULTIPLE USERS

Our convention will be that  $K$  users, each communicating from an M-ary signal set and a single-antenna transmitter, is communicating with an  $L$ -element receiver. The orthonormal basis for the  $KM$  symboling waveforms has cardinality  $N \leq KM$ . Then the basic model for multiple user communication with multiple receive antennas may be depicted as in Figure 1. At the  $l^{th}$  antenna element we receive the continuous-time signal

$$r_l(t) = \sum_{k=1}^K \alpha_l(k) s_{m_k}(t) + n_l(t), \quad (1)$$

where  $s_{m_k}(t)$  is the signal transmitted by user  $k$  from a set of cardinality  $M$ ,  $\alpha_l(k)$  is the fading coefficient for the path connecting user  $k$  to the  $l^{th}$  antenna, and  $n_l(t)$  is circularly symmetric complex Gaussian noise.

By matching to an  $N$ -dimensional orthonormal basis,  $\{u_n(t)\}_1^N$ , for the joint signal space spanned by all of the signals,  $\{s_{m_k}(t)\}$ , we build the measurement  $\mathbf{y}_l \in \mathbb{C}^N$ :

$$\mathbf{y}_l = \sum_{k=1}^K \alpha_l(k) \mathbf{h}_{m_k}(k) + \mathbf{n}_l = \sum_{k=1}^K \alpha_l(k) \mathbf{H}(k) \mathbf{b}(k) + \mathbf{n}_l. \quad (2)$$

<sup>1</sup>Michael McCloud and Mahesh Varanasi are with the Department of Electrical and Computer Engineering, University of Colorado, Boulder, CO, 80309-0425. Artur Russ is with Infineon Technologies, Munich, Germany. Louis Scharf is with the Departments of Electrical and Computer Engineering and Statistics, Colorado State University, Ft. Collins, CO 80523-1373.

This work was supported by the National Science Foundation under grants ANIR-9725778 and ECS-9979400, by the Office of Naval Research under Contract No. N00014-00-1-0033 and by the Army Research Office Grant No. DAAD 19-99-1-029.

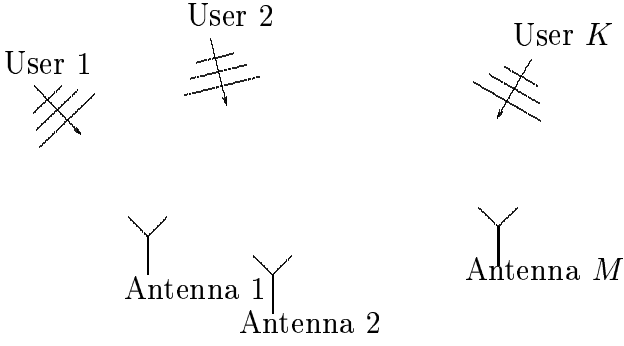


Figure 1: The antenna array model with multiple users.

Here  $\mathbf{h}_{m_k}(k)$  is a vector containing the expansion coefficients for the  $k^{\text{th}}$  user's  $m_k^{\text{th}}$  signal:

$$\{\mathbf{h}_{m_k}(k)\}_n = \int s_{m_k}(t) u_n^*(t) dt. \quad (3)$$

The matrix  $\mathbf{H} = [\mathbf{H}(1), \mathbf{H}(2), \dots, \mathbf{H}(K)]$  contains the signal vectors for each user with  $\mathbf{H}(k) = [\mathbf{h}_1(k), \mathbf{h}_2(k), \dots, \mathbf{h}_M(k)]$ . The vector  $\mathbf{b} = [\mathbf{b}^T(1), \mathbf{b}^T(2), \dots, \mathbf{b}^T(K)]^T$ , an  $MK \times 1$  vector with each  $\mathbf{b}(k)$  a column of the  $M \times M$  identity matrix, selects the signal transmitted by user  $k$ . That is,  $\mathbf{H}(k)\mathbf{b}_m(k) = \mathbf{h}_m(k)$ . The additive noise,  $\mathbf{n}_l \in \mathbb{C}^N$ , is a circularly symmetric white Gaussian vector with correlation  $E[\mathbf{n}_l \mathbf{n}_l^*] = \sigma^2 \mathbf{I}_N$ .

If we are interested in user  $k$ , we may rewrite our model with respect to this user as

$$y_l = \alpha_l \mathbf{h}_m + \mathbf{S} \boldsymbol{\rho}_l + \mathbf{n}_l, \quad (4)$$

where we have dropped the dependency on  $k$  and have collected all of the multiple access interference into the vector  $\mathbf{S} \boldsymbol{\rho}_l = \sum_{k' \neq k} \alpha_l(k') \mathbf{h}_{m_{k'}}(k')$ , i.e. the matrix  $\mathbf{S}$  contains all  $M(K-1)$  interfering signal vectors and the vector  $\boldsymbol{\rho}_l \in \mathbb{C}^{M(K-1)}$  is formed by stacking the vectors  $\alpha_l(k') \mathbf{b}(k')$  for  $k' \neq k$ .

We may now collect the measurements into the  $LN \times 1$  vector  $\mathbf{y} = [\mathbf{y}_1^T \mathbf{y}_2^T \dots \mathbf{y}_L^T]^T \in \mathbb{C}^{LN}$ :

$$\begin{aligned} \mathbf{y} &= \sum_{k=1}^K (\mathbf{I}_L \otimes \mathbf{H}(k)) (\boldsymbol{\alpha}(k) \otimes \mathbf{b}(k)) + \mathbf{n} \\ &= \mathcal{F} \mathbf{c} + \mathbf{n}, \end{aligned} \quad (5)$$

where  $\mathcal{F} = [\mathbf{I}_L \otimes \mathbf{H}(1) \dots \mathbf{I}_L \otimes \mathbf{H}(K)]$  contains all  $KLM$  of the users' space-time signalling vectors,  $\boldsymbol{\alpha}(k) = [\alpha_1(k) \dots \alpha_L(k)]^T$ , and

$$\mathbf{c} = \begin{bmatrix} \boldsymbol{\alpha}(1) \otimes \mathbf{b}(1) \\ \vdots \\ \boldsymbol{\alpha}(K) \otimes \mathbf{b}(K) \end{bmatrix}. \quad (6)$$

The symbol  $\otimes$  denotes the Kronecker product of two matrices (see e.g. [7]).

We can rewrite this model with respect to user  $k$  as

$$\begin{aligned} \mathbf{y} &= (\mathbf{I}_L \otimes \mathbf{h}_m) \boldsymbol{\alpha} + (\mathbf{I}_L \otimes \mathbf{S}) \boldsymbol{\rho} + \mathbf{n} \\ &= \mathcal{H}_m \boldsymbol{\alpha} + \mathbf{S} \boldsymbol{\rho} + \mathbf{n}, \end{aligned} \quad (7)$$

where  $\mathcal{H}_m = \mathbf{I}_L \otimes \mathbf{h}_m$ ,  $\mathbf{S} = \mathbf{I}_L \otimes \mathbf{S}$ , and  $\boldsymbol{\rho} = [\boldsymbol{\rho}_1^T, \dots, \boldsymbol{\rho}_L^T]^T \in \mathbb{C}^{LM(K-1)}$ .

We note that the measurement space has dimension  $LN$ , whereas the signal and interference lie in subspaces of respective dimensions  $L$  and  $L(K-1)$ . We see that low space dimension  $L$  can be compensated by large time dimension  $N$ , or vice-versa, for separating signal and interference.

### III. COHERENT WAVEFRONT FADING

We first consider the special case of phase coherent fading, meaning that the fading parameters for each user are modeled as  $\alpha_l(k) = \alpha(k) a_l(\theta_k)$ , where  $\alpha(k)$  is a constant complex fading parameter across the array,  $\theta_k$  is the direction of arrival of the  $k^{\text{th}}$  user's signal relative to the array geometry, and  $a_l(\theta_k)$  is the response of the  $l^{\text{th}}$  sensor to a narrow-band signal arriving from  $\theta_k$ . See e.g. [8] for a more detailed development of this model.

In this case the model of equation 5 simplifies to

$$\mathbf{y} = \sum_{k=1}^K \alpha(k) (\mathbf{I}_L \otimes \mathbf{h}_{m_k}(k)) \mathbf{a}(\theta_k) + \mathbf{n}. \quad (8)$$

If the direction of arrival for each of the users is known we may simplify our model with respect to user  $k$  as

$$\mathbf{y} = \alpha \mathbf{h}_m + \mathbf{S} \boldsymbol{\beta} + \mathbf{n}, \quad (9)$$

where bold-script  $\mathbf{h}_m(k)$  is the following signal vector, defined by its symboling vector  $\mathcal{H}_m(k)$  and its arrival angle  $\theta_k$ :

$$\mathbf{h}_m(k) = (\mathbf{I}_L \otimes \mathbf{h}_m(k)) \mathbf{a}(\theta_k) = \mathcal{H}_m \mathbf{a}(\theta_k), \quad (10)$$

$\mathbf{S}$  is the matrix containing the  $(K-1)M$  interference vectors  $\{\mathbf{h}_{m_{k'}}(k')\}$  for  $k' \neq k$ , and  $\boldsymbol{\beta}$  is formed by stacking the vectors  $\alpha(k') \mathbf{b}(k')$  for  $k' \neq k$ ; i.e.  $\mathbf{S} \boldsymbol{\beta} = \sum_{k' \neq k} \alpha(k') \mathbf{h}_{m_{k'}}(k')$ . Notice that  $\{\mathbf{h}_m(k)\}$ , the DOA resolved signals, should not be confused with  $\{\mathbf{h}_m(k)\}$ , the original time signals. Except for the very important details about the space-time structure of  $\mathbf{h}_m$  and  $\mathbf{S}$ , our model is now algebraically identical to that considered in [2]-[4] and the detectors contained there may be used on this channel without modification. The interference matrix,  $\mathbf{S}$ , is the *space-time* (or more accurately the *space-dimension*) matrix formed by the vectors  $(\mathbf{I}_L \otimes \mathbf{h}_{m_{k'}}(k')) \mathbf{a}(\theta_{k'})$  for  $k' \neq k$ . If we choose the basis functions to be time delayed versions of a common pulse shape (for instance in direct sequence-code division multiple access (DS-SS) or time-division multiple access (TDMA) communications), we can consider  $\mathbf{S}$  to be the *space-time* interference matrix. In general, the basis functions need not have such an interpretation (they could be chosen to efficiently manage bandwidth, for example).

#### A The Generalized Maximum Likelihood (GML) Detector

The first detector that we consider is the generalized maximum likelihood (GML) rule developed in [2]-[4] by maximizing the likelihood functions

$$f_m(\mathbf{y}) = \frac{1}{(\pi\sigma^2)^{LN}} \exp \left\{ \frac{1}{\sigma^2} \|\mathbf{y} - \mathbf{h}_m \alpha - \mathbf{S} \boldsymbol{\beta}\|^2 \right\} \quad (11)$$

over the unknown parameters  $\boldsymbol{\beta}$  and  $\alpha$ . The result is

$$\hat{m}_{GML} = \arg \max_m \frac{|\mathbf{y}^* \mathbf{P}_{\mathbf{S}}^{\perp} \mathbf{h}_m|^2}{\|\mathbf{P}_{\mathbf{S}}^{\perp} \mathbf{h}_m\|^2} = \arg \max_m \mathbf{y}^* \mathbf{P}_{\mathbf{S}} \mathbf{h}_m \mathbf{y}. \quad (12)$$

The right-most form of equation (12) shows the GML detector to be a matched subspace detector [9]. The GML detector

chooses the signal,  $\mathbf{h}_m$ , which has the greatest direction cosine with the measurement in the subspace orthogonal to the interference,  $\langle \mathbf{S} \rangle^\perp$ . This detector is *invariant* to complex scaling of the data and to translations of the data in the interference subspace,  $\langle \mathbf{S} \rangle$ . A more thorough discussion of the geometry and invariances of the GML detector is presented in [3].

The GML detector for waveform fading bears comment, for it reveals an important decomposition of the space-time receiver. To make this point, let us rewrite the quadratic form in (12) as

$$\arg \max_m \mathbf{y}^* \mathbf{P}_{\mathbf{P}_S^\perp \mathbf{h}_m} \mathbf{y} = \arg \max_m \frac{|\mathbf{a}(\theta_k)^* (\mathbf{I}_L \otimes \mathbf{h}_m)^* \mathbf{P}_S^\perp \mathbf{y}|^2}{\mathbf{a}(\theta_k)^* (\mathbf{I}_L \otimes \mathbf{h}_m)^* \mathbf{P}_S^\perp (\mathbf{I}_L \otimes \mathbf{h}_m) \mathbf{a}(\theta_k)}. \quad (13)$$

The implementation of this ratio of quadratic forms is illustrated in Figure 2. It consists of a space-time interference rejection operator  $\mathbf{P}_S^\perp$ , followed by temporal matched filtering and then spatial matched filtering (beamforming). Note that there is no approximation in this factored implementation of the space-time GML detector.

### B The Multiple Antenna Minimum Mean Squared Error (MMSE) and the Decorrelating Detectors

We next consider the minimum mean square error (MMSE) detector for M-ary modulation in [3] and [4] (and also discussed in [10]):

$$\hat{m}_{MMSE} = \arg \max_m \left\{ \left| \mathbf{h}_m^* \mathbf{R}^{-1} \mathbf{y} \right|^2 \right\}, \quad (14)$$

where  $\mathbf{R} = E[\mathbf{y}\mathbf{y}^*] \in \mathbb{C}^{LN \times LN}$ . As the SNR grows large, we find that the MMSE detector converges to the zero-forcing multipulse decorrelating (MD) detector derived in [4]:

$$\hat{m}_{MD} = \arg \max_m \left\{ \left| \left( \mathbf{H}^* \mathbf{P}_S^\perp \mathbf{H} \right)^+ \mathbf{H}^* \mathbf{P}_S^\perp \mathbf{y} \right|^2 \right\}. \quad (15)$$

Here  $\mathbf{H} = [\mathbf{h}_1 \cdots \mathbf{h}_M]$ , with the  $\mathbf{h}_m$  defined in equation (10), are the angle-resolved signal vectors for the user of interest. This detector is generally not the GML detector, except when the matrix  $\mathbf{h}^* \mathbf{P}_S^\perp \mathbf{h}$  is diagonal, a point which is discussed in [4].

### C Performance of the Detectors

The performance of the GML and MMSE detectors has been analyzed on the noncoherent additive white Gaussian noise channel in [2]-[4]. In this section we will extend this analysis to the Rayleigh fading channel. We will employ the union bound on the probability of error,

$$P \leq \frac{1}{M} \sum_{m=1}^M \sum_{\substack{l=1 \\ l \neq m}}^M P(m, l), \quad (16)$$

where  $P(m, l)$  is the probability that the  $l^{\text{th}}$  decision statistic is greater than the  $m^{\text{th}}$  statistic when signal  $m$  is transmitted. We derive asymptotic (in the SNR) expressions for these bounds, so we will only consider the zero-forcing detectors (GML and MD), as the MMSE detector converges to the MD detector at high SNRs. We will need expressions for the two-signal error probability for each detector, and these are computed in the following paragraphs.

### C.1 The GML Detector

The pairwise probability of error is

$$P_{GML}(m, l) = \text{Prob} \left[ \frac{|\mathbf{y}^* \mathbf{P}_S^\perp \mathbf{h}_m|^2}{\|\mathbf{P}_S^\perp \mathbf{h}_m\|^2} < \frac{|\mathbf{y}^* \mathbf{P}_S^\perp \mathbf{h}_l|^2}{\|\mathbf{P}_S^\perp \mathbf{h}_l\|^2} \right] \quad (17)$$

when signal  $\mathbf{h}_m$  was transmitted. Letting  $\mathbf{P}_m = \mathbf{P}_{\mathbf{P}_S^\perp \mathbf{h}_m}$ ,  $\mathbf{P}_l = \mathbf{P}_{\mathbf{P}_S^\perp \mathbf{h}_l}$  and  $\Delta_{\mathbf{P}} = \mathbf{P}_m - \mathbf{P}_l$ , we have

$$P_{GML}(m, l) = \text{Prob}[\mathbf{y}^* \Delta_{\mathbf{P}} \mathbf{y} < 0]. \quad (18)$$

Using the results of [11, Appendix B] we find the characteristic function of the quadratic form  $z = \mathbf{y}^* \Delta_{\mathbf{P}} \mathbf{y}$  to be

$$G_z(s) = \frac{1}{\det(\mathbf{I} + s(\gamma^2 \mathbf{P}_S^\perp \mathbf{h}_m \mathbf{h}_m^* \mathbf{P}_S^\perp + \sigma^2 \mathbf{I}) \Delta_{\mathbf{P}})}, \quad (19)$$

where  $\gamma^2 = E[|\alpha(k)|^2]$  is the variance of the wavefront fade for user  $k$ .

To determine the probability of error, we need to find the two nonzero eigenvalues,  $\lambda^{GML}$ , of the matrix  $(\gamma^2 \mathbf{P}_S^\perp \mathbf{h}_m \mathbf{h}_m^* \mathbf{P}_S^\perp + \sigma^2 \mathbf{I}) \Delta_{\mathbf{P}}$ . The corresponding error probability is then

$$P_{GML}(m, l) = \frac{1}{(1 - \lambda_2^{GML} / \lambda_1^{GML})}, \quad (20)$$

where we have identified  $\lambda_1^{GML}$  as the positive eigenvalue (see e.g. [5, 12, 13] for more information on symbol error probabilities and their asymptotic behavior for the fading channel).

By solving for these eigenvalues and determining their asymptotic form (through a Taylor series about  $\sigma^2 = 0$ ) we find the large SNR bound for the GML performance. The corresponding asymptotic expression for the pairwise error probabilities is

$$P_{GML}(m, l) \sim \frac{1}{1 + SNR_{GML}}, \quad (21)$$

where  $SNR_{GML}$  is the following signal-to-noise ratio:

$$SNR_{GML} = \left( \frac{\gamma^2 \|\mathbf{h}_m\|^2}{\sigma^2} \right) \sin^2(\mathbf{h}_m, \mathbf{S}) \sin^2(\mathbf{P}_S^\perp \mathbf{h}_m, \mathbf{P}_S^\perp \mathbf{h}_l). \quad (22)$$

We notice that the probability of error is a function of this effective SNR, which relates the geometry of the signal set directly to the asymptotic performance of the detector through the sine-squared terms  $\sin^2(\mathbf{P}_S^\perp \mathbf{h}_m, \mathbf{P}_S^\perp \mathbf{h}_l)$  and  $\sin^2(\mathbf{h}_m, \mathbf{S})$ .

### C.2 The MD Detector

For the MD detector (and hence the MMSE detector at large SNRs) we find

$$P_{MD}(m, l) = \text{Prob} \left[ \mathbf{y}^* \mathbf{P}_S^\perp \mathbf{H} \left( \mathbf{H}^* \mathbf{P}_S^\perp \mathbf{H} \right)^+ (\mathbf{e}_m \mathbf{e}_m^T - \mathbf{e}_l \mathbf{e}_l^T) \left( \mathbf{H}^* \mathbf{P}_S^\perp \mathbf{H} \right)^+ \mathbf{H}^* \mathbf{P}_S^\perp \mathbf{y} < 0 \mid \text{Hyp. } m \right],$$

where  $\mathbf{e}_m$  is the  $m^{\text{th}}$  column of the identity matrix. We seek the two nonzero eigenvalues of the matrix

$$\mathbf{R}_{\mathbf{y}\mathbf{y}} (\mathbf{Q}^* (\mathbf{e}_m \mathbf{e}_m^T - \mathbf{e}_l \mathbf{e}_l^T) \mathbf{Q}), \quad (23)$$

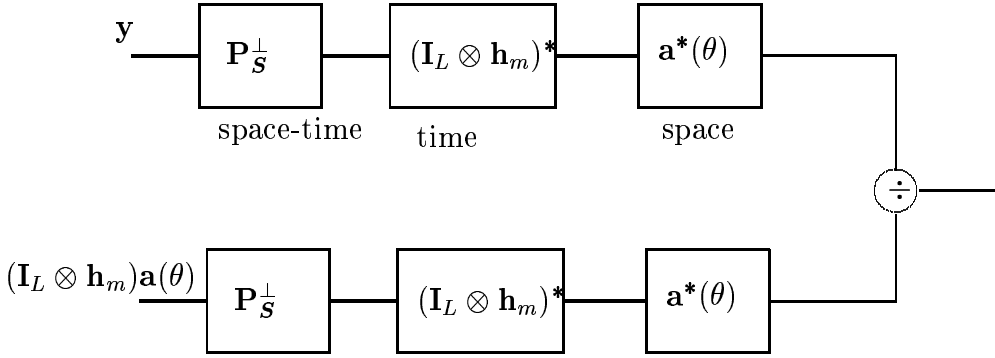


Figure 2: Space-time structure of the GML detector.

where  $\mathbf{Q} = (\mathbf{H}^* \mathbf{P}_S^\perp \mathbf{H})^\dagger \mathbf{H}^* \mathbf{P}_S^\perp$ .

For the case of linearly independent signals ( $\mathbf{H}^* \mathbf{P}_S^\perp \mathbf{H}$  full rank), we find the following asymptotic form of the error bound (where we expanded  $\lambda_{1,2}^{M,D}$  in a Taylor series around  $\sigma^2 = 0$  and kept only the linear term)

$$P^{MD}(m, l) \sim \frac{1}{1 + SNR_{MD}}, \quad (24)$$

where  $SNR_{MD}$  is the effective signal-to-noise ratio:

$$SNR_{MD} = \left( \frac{\gamma^2}{\sigma^2} \right) \frac{1}{(\mathbf{H}^* \mathbf{P}_S^\perp \mathbf{H})_{l,l}^{-1}}. \quad (25)$$

#### D A Numerical Example

We now consider an example of multiuser communications on the wavefront fading channel. We have  $K = 2$  users, each employing  $M = 2$  signals with a processing gain of  $N = 3$ . A uniform linear array was employed with half wavelength sensor spacing and  $L = 3$  sensors. The fading processes for each user were assumed to have the same variance and the users employed identical waveform signalling, meaning that the two users employ exactly the same signals, i.e.  $\mathbf{H}(1) = \mathbf{H}(2)$ . For this case, all of the interference rejection comes from beamforming. This is sometimes called angle-division multiple access (ADMA). Notice that bandwidth can be easily managed in this scheme as each user employs exactly the same frequency band; users can be added without increasing the bandwidth so long as there are enough sensors in the array to resolve the users' DOAs. Since the signal separation between the two users is only a function of their arrival angles, we fixed user one's DOA to  $50^\circ$  and varied the interfering user's DOA from  $-90^\circ$  to  $90^\circ$ . The SNR was fixed at 20dB. The results of this experiment are shown in Figure 3, and we notice that when the interfering user is close to the desired user the performance degradation is severe, as expected.

#### IV. NONCOHERENT ELEMENT-TO-ELEMENT FADING

In the case of element-to-element fading we allow the fading parameters to change across the face of the array. In this case, the dependency of the array response on the direction of arrival for each user can not be separated from the fading process, and we consequently subsume its effects into the fading. No beamforming is possible. We return to the general measurement model of equation (7),

$$\mathbf{y} = \mathcal{H}_m \boldsymbol{\alpha} + \mathcal{S} \boldsymbol{\rho} + \mathbf{n},$$

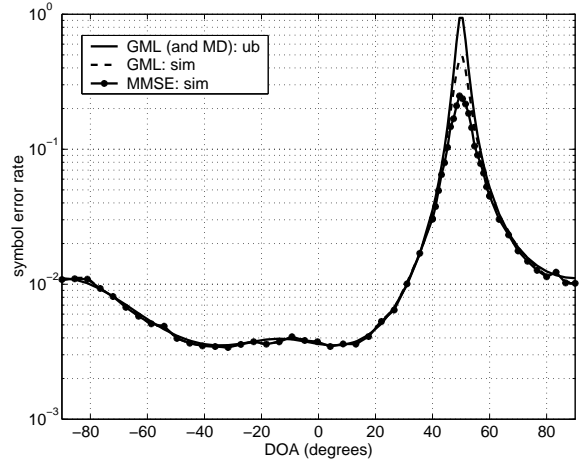


Figure 3: Symbol error rate versus direction of arrival of the interfering user for the GML and MMSE detectors with identical waveform signalling.

#### A Generalized Likelihood Detection

The first detector that we consider models the fading parameters,  $\boldsymbol{\alpha}$ , as unknown deterministic quantities and is *invariant* to their effects. If we knew the multiple access interference (MAI) and the fading for the user of interest the optimal detector would form the  $M$  likelihood functions

$$f_m(\mathbf{y}|\boldsymbol{\alpha}, \boldsymbol{\rho}) = \frac{1}{(\pi\sigma^2)^{LN}} \exp \left\{ \frac{-1}{\sigma^2} \|\mathbf{y} - \mathcal{H}_m \boldsymbol{\alpha} - \mathcal{S} \boldsymbol{\rho}\|^2 \right\}. \quad (26)$$

The corresponding decision,  $\hat{m}(k)$  is the argument which maximizes these functions for each user  $k$ . In our model we do not know  $\boldsymbol{\alpha}$  and  $\boldsymbol{\rho}$  and consequently need to find an alternative approach. To form the GML detector, we build maximum likelihood estimates of these quantities under each hypothesis and employ the test

$$\hat{m}_{GML} = \arg \max_m f_m(\mathbf{y}|\hat{\boldsymbol{\alpha}}, \hat{\boldsymbol{\rho}}). \quad (27)$$

By employing the usual Kronecker identities (see e.g. [7]), it can be shown that the GML detector is given by

$$\hat{m}_{GML} = \arg \max_m \sum_{l=1}^L \mathbf{y}_l^* \mathbf{P}_{\mathbf{P}_S^\perp \mathbf{h}_m} \mathbf{y}_l. \quad (28)$$

### B A Minimum Mean Squared Error Detection Rule

We now place the complex normal distribution on each vector,  $\mathbf{\alpha}$ , to model Rayleigh fading. We shall assume the users' fading paths are mutually uncorrelated, each with zero mean and correlation  $\mathbf{R}_{\alpha\alpha}(k)$ . We return to the model of equation (5),

$$\mathbf{y} = \mathcal{F}\mathbf{c} + \mathbf{n},$$

and notice that the measurement is zero mean with correlation  $\mathbf{R}_{\mathbf{y}\mathbf{y}} = \mathcal{F}\mathbf{R}_{\mathbf{c}\mathbf{c}}\mathcal{F}^* + \sigma^2\mathbf{I}$ , where  $\mathbf{R}_{\mathbf{c}\mathbf{c}} = \text{diag}\{(1/M)\mathbf{R}_{\alpha\alpha}(k) \otimes \mathbf{I}_M\}$ .

We propose to first form the minimum mean squared error estimate of the vector  $\mathbf{c}$ , and use its  $k^{\text{th}}$  sub-block,  $\hat{\mathbf{c}}(k)$ , to form the decision

$$\hat{m}_{MMSE} = \arg \max_m \sum_{l=1}^L \left| \{\hat{\mathbf{c}}(k)\}_{M(l-1)+m} \right|^2. \quad (29)$$

This detector is motivated by the fact that under hypothesis  $m$  the vector  $\mathbf{c}(k)$  has non-zero entries only in these positions. We compute the MMSE estimate of  $\mathbf{c}$  using standard second order statistical theory and find

$$\hat{\mathbf{c}} = \mathbf{R}_{\mathbf{c}\mathbf{c}}\mathcal{F}^* \left( \mathcal{F}\mathbf{R}_{\mathbf{c}\mathbf{c}}\mathcal{F}^* + \sigma^2\mathbf{I} \right)^{-1} \mathbf{y}. \quad (30)$$

Taking the  $k^{\text{th}}$  sub-block yields the statistic

$$\hat{\mathbf{c}}(k) = \frac{1}{M} \left( \mathbf{R}_{\alpha\alpha}(k) \otimes \mathbf{I}_M \right) \mathcal{H}_m^* \left( \mathcal{F}\mathbf{R}_{\mathbf{c}\mathbf{c}}\mathcal{F}^* + \sigma^2\mathbf{I} \right)^{-1} \mathbf{y}, \quad (31)$$

which can be used in the detector of equation 29.

### C Independent Fading

We examine the special case of independent fading, meaning that the  $L$  paths are uncorrelated for each user. In this case we have  $\mathbf{R}_{\alpha\alpha}(k) = \Gamma^2(k)$ , a diagonal matrix. Under this model we find that the measurement has correlation

$$\begin{aligned} \mathbf{R}_{\mathbf{y}\mathbf{y}} &= \sum_{k=1}^K \text{diag} \left\{ \frac{\gamma_l^2(k)}{M} \mathbf{H}(k)\mathbf{H}(k)^* \right\} + \sigma^2\mathbf{I} \\ &= \text{diag} \{ \mathbf{R}_{\mathbf{y}_l\mathbf{y}_l} \}. \end{aligned} \quad (32)$$

The corresponding MMSE test is simply

$$\hat{m}_{MMSE}(k) = \arg \max_m \sum_{l=1}^L \left( \gamma_l^2(k) \right)^2 \left| \mathbf{h}_m^*(k) \mathbf{R}_{\mathbf{y}_l\mathbf{y}_l}^{-1} \mathbf{y}_l \right|^2, \quad (33)$$

which is the average of  $L$  single-antenna MMSE detection statistics of the type presented in [3] and [4], with the weights determined by the channel fading powers,  $\{\gamma_l^2(k)\}$ .

### D The Multiple Antenna Decorrelating Detector

In [4] we analyzed the single-antenna MMSE detector as the SNR grew large and suggested that the asymptotic form of that detector be called the multipulse decorrelating detector (MD). A similar analysis is possible for the multiple sensor MMSE estimator of equation 31. Employing the same algebraic steps as in [4], we find that asymptotically:

$$\hat{\mathbf{c}}(k) \rightarrow \left( \mathcal{H}^* \mathbf{P}_S^\perp \mathcal{H} \right)^+ \mathcal{H}^* \mathbf{P}_S^\perp \mathbf{y}, \quad (34)$$

where  $\mathbf{S}$  is the interference matrix defined in equation 7 and we have dropped the dependence on  $k$ .

We may apply the properties of the Kronecker product to find that

$$\begin{aligned} \left( (\mathbf{I}_L \otimes \mathbf{H})^* \mathbf{P}_S^\perp (\mathbf{I}_L \otimes \mathbf{H}) \right)^+ (\mathbf{I}_L \otimes \mathbf{H})^* \mathbf{P}_S^\perp \mathbf{y} &= \\ \left( \mathbf{I}_L \otimes \left( \mathbf{H}^* \mathbf{P}_S^\perp \mathbf{H} \right)^+ \mathbf{H}^* \mathbf{P}_S^\perp \right) \mathbf{y}. \end{aligned} \quad (35)$$

The MD test is therefore given by

$$\hat{m}_{MD} = \arg \max_m \sum_{l=1}^L \left| \left\{ \left( \mathbf{H}^* \mathbf{P}_S^\perp \mathbf{H} \right)^+ \mathbf{H}^* \mathbf{P}_S^\perp \mathbf{y}_l \right\}_m \right|^2, \quad (36)$$

which is the sum of  $L$  single-antenna MD statistics. It is interesting to notice that, like the GML test, the MD detector is invariant to the multiple access interference and does not use the spatial structural information contained in  $\mathbf{R}_{\alpha\alpha}(k)$  to make its decision.

### E Performance of the Detectors

We proceed as in Section C and employ union upper bounds to quantify the performance of the detection rules. This means that we need to determine the pairwise error probabilities for each pair of signals. We make use of the fact that, for each detector, an error occurs when a certain quadratic form  $\mathbf{y}^* \mathbf{A} \mathbf{y}$  is negative. The kernel,  $\mathbf{A}$ , is different for each detector. For the Rayleigh fading channel, the performance is a function of the eigenvalues,  $\lambda_k$ , of the matrix  $\mathbf{R}_{\mathbf{y}\mathbf{y}} \mathbf{A}$ . We will consider the zero-forcing detectors (GML and MD) so we may employ the interference-nulled measurement  $\mathbf{z} = \mathcal{W}^* \mathbf{y}$  with the correlation matrix  $\mathbf{R}_{\mathbf{z}\mathbf{z}} = \mathcal{G}_m \mathbf{R}_{\alpha\alpha} \mathcal{G}_m^* + \sigma^2 \mathbf{I}$  when user  $k$  transmits its  $m^{\text{th}}$  signal, where we have factored the interference projection matrix as  $\mathbf{P}_S = \mathcal{W} \mathcal{W}^*$  and defined  $\mathcal{G}_m = \mathcal{W}^* \mathcal{H}_m$ . Given the eigenvalues, the union bound is given by

$$P(m, l) = - \sum_{\lambda_k < 0} \text{Res} \left( \frac{1}{s \prod_{l=1}^{2L} \lambda_l \left( s + \frac{1}{\lambda_l} \right)}, s_k = -\frac{1}{\lambda_k} \right), \quad (37)$$

where we sum over the residues of the negative eigenvalues (see e.g. [12],[14], [13]).

## V. SUMMARY AND CONCLUSIONS

We summarize our key findings by reviewing the GML and MD detectors for wavefront and element-to-element fading in Table 1. In this table  $\mathbf{h}_m = (\mathbf{I}_L \otimes \mathbf{h}_m) \mathbf{a}(\theta)$ ,  $\mathcal{H}_m = (\mathbf{I}_L \otimes \mathbf{h}_m)$ ,  $\mathbf{H} = [\mathbf{h}_1 \cdots \mathbf{h}_M]$ ,  $\mathbf{S} = (\mathbf{I}_L \otimes \mathbf{S}) [\mathbf{a}(\theta_1) \cdots \mathbf{a}(\theta_K)]$  excluding  $\mathbf{a}(\theta_k)$ , and  $\mathcal{S} = (\mathbf{I}_L \otimes \mathcal{S})$ . That is,  $\mathbf{h}_m = \mathcal{H}_m \mathbf{a}(\theta)$  and  $\mathcal{S} = \mathcal{S} \mathbf{A}$  for  $\mathbf{A} = [\mathbf{a}(\theta_1) \cdots \mathbf{a}(\theta_K)]$ , excluding  $\mathbf{a}(\theta_k)$ .

We see that the crucial difference between the two models is that the wavefront fading we may associate a direction of arrival,  $\theta_k$ , to each user and exploit this structure to form a one-dimensional matched subspace detector which performs spatial beamforming and temporal matched filtering separately. For the case of element-to-element fading we match to an  $L$ -dimensional subspace,  $\mathcal{H}(k)$ . More importantly, we are forced to project onto the  $(N-(K-1)L)$ -dimensional subspace  $\langle \mathcal{S} \rangle^\perp$  on the element-to-element channel while we employed the larger  $(N-(K-1))$ -dimensional subspace  $\langle \mathbf{S} \rangle^\perp$  for the wavefront fading channel. Of course, the element-to-element fading channel allows for several diversity branches in the receiver, allowing for robustness to the Rayleigh fading.

Fading	GML	MD
wavefront	$\arg \max_m \mathbf{y}^* \mathbf{P}_{\mathbf{P}_S^\perp \mathbf{h}_m} \mathbf{y}$	$\arg \max_m \left\  \left\{ (\mathbf{H}^* \mathbf{P}_S^\perp \mathbf{H})^\dagger \mathbf{H}^* \mathbf{P}_S^\perp \mathbf{y} \right\}_m \right\ ^2$
element-to-element	$\arg \max_m \mathbf{y}^* \mathbf{P}_{\mathbf{P}_S^\perp \mathbf{h}_m} \mathbf{y}$ $= \arg \max_m \sum_{l=1}^L \mathbf{y}_l^* \mathbf{P}_{\mathbf{P}_S^\perp \mathbf{h}_m} \mathbf{y}_l$	$\arg \max_m \sum_{l=1}^L \left\  \left\{ (\mathbf{H}^* \mathbf{P}_S^\perp \mathbf{H})^\dagger \mathbf{H}^* \mathbf{P}_S^\perp \mathbf{y}_l \right\}_m \right\ ^2$

Table 1: Summary of detectors.

## References

- [1] M. K. Varanasi, "Noncoherent detection in asynchronous multiuser channels," *IEEE Trans. Inform. Theory*, vol. IT-39, no. 1, pp. 157–176, Jan. 1993.
- [2] M. K. Varanasi and A. Russ, "Noncoherent decorrelative detection for nonorthogonal multipulse modulation over the multiuser Gaussian channel," *IEEE Trans. Commun.*, vol. 46, no. 12, pp. 1675–1684, Dec. 1998.
- [3] M. L. McCloud and L. L. Scharf, "Interference estimation with applications to blind multiple-access communication over fading channels," *IEEE Trans. Inform. Theory*, vol. 46, no. 3, pp. 947–961, May 2000.
- [4] M. L. McCloud and L. L. Scharf, "Asymptotic analysis of the MMSE multiuser detector for non-orthogonal multipulse modulation," *IEEE Trans. Commun.*, vol. 49, no. 1, pp. 24–30, Jan. 2001.
- [5] A. Russ and M. K. Varanasi, "Noncoherent multiuser detection for nonlinear modulation over the Rayleigh fading channel," *IEEE Trans. Inform. Theory*, vol. 47, no. 1, pp. 295–307, Jan. 2001.
- [6] M. K. Varanasi and D. Das, "Noncoherent decision feedback multiuser detection: Optimality, performance bounds, and rules for ordering users," in *Proc. IEEE Intl. Symposium on Information Theory*, Aug. 1998, p. 35.
- [7] R. A. Horn and C. R. Johnson, *Topics in Matrix Analysis*, Cambridge University Press, New York, 1994.
- [8] P. Stoica and R. Moses, *Introduction to Spectral Analysis*, Simon and Schuster, Upper Saddle River, NJ, 1997.
- [9] L. L. Scharf and B. Friedlander, "Matched subspace detectors," *IEEE Trans. Signal Processing*, vol. 42, no. 8, pp. 2146–2157, 1994.
- [10] A. Kapur, D. Das, and M. K. Varanasi, "Noncoherent MMSE multiuser receivers for non-orthogonal multipulse modulation and blind adaptive algorithms," in *Proc. Conf. Inform. Sciences and Systems*. Princeton University, Mar. 2000, pp. FP3.13–FP3.18.
- [11] M. Schwartz, W. R. Bennett, and S. Stein, *Communication Systems and Techniques*, An IEEE Press Classic Reissue, New York, 1996, Originally A McGraw-Hill Publication, 1966.
- [12] E. Biglieri, H. L. Owen, and E. W. Zegura, "Computing error probabilities over fading channels: A unified approach," *European Trans. on Telecommun.*, vol. 9, no. 1, Feb. 1998.
- [13] M. Brehler and M. K. Varanasi, "Asymptotic error probability analysis of quadratic receivers in Rayleigh fading channels with applications to a unified analysis of coherent and noncoherent space-time receivers," submitted to *IEEE Trans. Inform. Theory*, Aug. 2000, accepted for publication.
- [14] A. Russ and M. K. Varanasi, "Noncoherent multiuser detection for CDMA mobile communication," Tech. Rep., University of Colorado, May 1997, also a Dipl.-Ing. thesis submitted to the Friedrich–Alexander–Universität.